

RESIDUAL SIGNAL IN SUB-BAND ACOUSTIC ECHO CANCELLERS

O. Tanrikulu, B. Baykal, A. G. Constantinides and J. A. Chambers

Sig. Proc. & Dig. Syst. Sec., Dept. of EE. Eng.,
Imperial College of Sci., Tech. and Med., London SW7 2BT, UK.

Email: o.tanrikulu@ic.ac.uk, Fax: + 44 171 594 6234

ABSTRACT

All-pass based Power Symmetric QMF-IIR (PS-QMF-IIR) and Aliasing Cancellation QMF-FIR (AC-QMF-FIR) sub-band decomposition approaches are studied in the context of Acoustic Echo Cancellation. The properties of the residual echo signal are obtained. For both filter types, if the filters have very sharp transition-bands, the residual echo signal contains tonal components. It is shown that these can be efficiently removed by using notch filters. Experimental results indicate that PS-QMF-IIR filters are better suited for this application than FIR filter based sub-band approaches, when combined with the notch filters presented.

1 INTRODUCTION

Acoustic Echo Cancellation (AEC) is a critical problem in hands-free voice communication systems such as in mobile telephony and audio teleconferencing [2, 5]. In AEC, acoustic echos are generated from the far-end speech by the acoustic coupling at the near-end. The objective is to avoid the propagation of echo to the far-end speaker. This is illustrated in Figure 1. Efficient suppression of the echo demands high

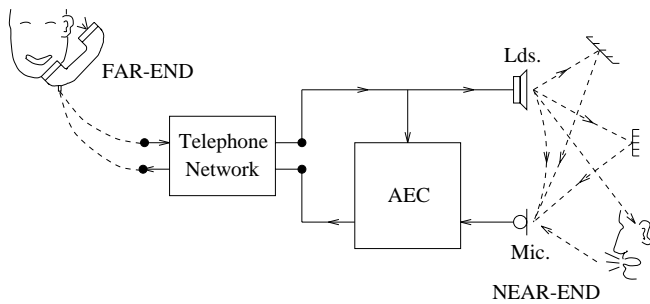


Figure 1: Acoustic Echo Cancellation.

computational power since the acoustic echo path impulse response is generally quite long, in the order of hundreds to thousands. Sub-band processing approaches offer a significant reduction in computational complexity but they have some limitations. These are; (1) the delay introduced to the system which is critical in application environments such as GSM, (2) the computational complexity introduced by the sub-band decomposition itself, and most importantly (3) the aliasing of the sub-band signals after decomposition. In this paper, we concentrate on the structure in Figure 2, where there are two sub-bands. However, our conclusions are valid

if more sub-bands are used. Gilloire and Vetterli [2] carried

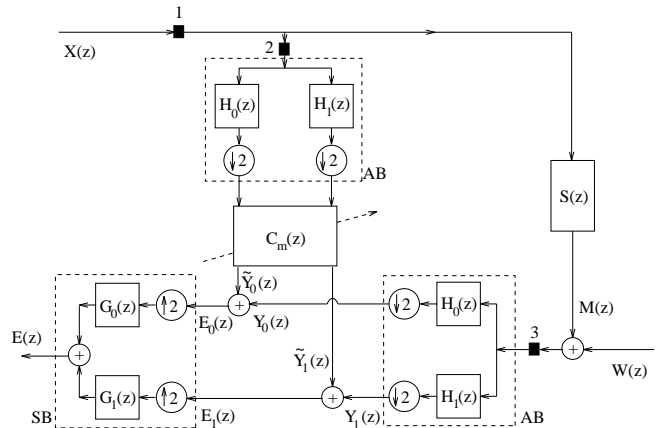


Figure 2: Sub-band Acoustic Echo Cancellation. AB: Analysis Bank, SB: Synthesis Bank

out a detailed analysis of this structure. They concentrate on Finite Impulse Response (FIR) multi-rate filter banks with Aliasing Cancelling (AC) or Perfect Reconstruction (PR) property. They have shown that even if the Analysis and Synthesis Banks satisfy the PR property, the aliasing present after sub-band decomposition is a serious problem for the identification of the acoustic echo path characteristics. They proposed to predict adaptively neighbouring sub-bands signals which we refer to as Cross-Channel Identification (CCI). This is feasible in a deterministic setting but when adaptive filters are used on-line, such an approach decreases the convergence speed and increases the computational complexity to an undesirable level.

We concentrate on the case where CCI is not used, that is when each sub-band echo signal is predicted from the corresponding loudspeaker signal only. The motivation is to deal with the aliasing problem by using highly selective All-pass based PS-QMF-IIR filter banks [3, 5]. In this paper, we extend our discussion to examine the properties of the residual echo signal, $E(z)$, when CCI is not used. For this purpose, we assume that the near-end speaker is inactive, i.e. $W(z) = 0$. The loudspeaker and the corresponding echo signals are respectively denoted by $X(z)$ and $M(z)$. The acoustic echo-path impulse response is shown as $S(z)$. We

use the Modulation-Domain Notation in [2] and define

$$\mathbf{x}_m(z) = [X(z)X(-z)]^T \quad (1)$$

$$\mathbf{S}_m(z) = \begin{bmatrix} S(z) & 0 \\ 0 & S(-z) \end{bmatrix} \quad (2)$$

$$\mathbf{H}_m(z) = \begin{bmatrix} H_0(z) & H_0(-z) \\ H_1(z) & H_1(-z) \end{bmatrix} \quad (3)$$

$$\mathbf{g}_m(z) = [G_0(z)G_1(z)]^T \quad (4)$$

$$\mathbf{C}_m(z) = \begin{bmatrix} C_{0,0}(z) & C_{0,1}(z) \\ C_{1,0}(z) & C_{1,1}(z) \end{bmatrix} \quad (5)$$

$$\mathbf{y}_m(z) = \begin{bmatrix} Y_0(z) \\ Y_1(z) \end{bmatrix} = \frac{1}{2}\mathbf{H}_m(z^{1/2})\mathbf{S}_m(z^{1/2})\mathbf{x}_m(z^{1/2}) \quad (6)$$

$$\tilde{\mathbf{y}}_m(z) = \begin{bmatrix} \tilde{Y}_0(z) \\ \tilde{Y}_1(z) \end{bmatrix} = \frac{1}{2}\mathbf{C}_m(z)\mathbf{H}_m(z^{1/2})\mathbf{x}_m(z^{1/2}) \quad (7)$$

$$\begin{aligned} E(z) &= \mathbf{g}_m^T(z)(\mathbf{y}_m(z^2) - \tilde{\mathbf{y}}_m(z^2)) \\ &= \frac{1}{2}\mathbf{g}_m^T(z)(\mathbf{H}_m(z)\mathbf{S}_m(z) - \mathbf{C}_m(z^2)\mathbf{H}_m(z))\mathbf{x}_m(z) \end{aligned} \quad (8)$$

Therefore, the residual error $E(z)$ is zero if

$$\mathbf{C}_m(z^2) = \mathbf{H}_m(z)\mathbf{S}_m(z)[\mathbf{H}_m(z)]^{-1} \quad (9)$$

$$[\mathbf{H}_m(z)]^{-1} = \frac{1}{\det[\mathbf{H}_m(z)]} \begin{bmatrix} H_1(-z) & -H_0(-z) \\ -H_1(z) & H_0(z) \end{bmatrix} \quad (10)$$

2 ALL-PASS BASED PS-QMF-IIR FILTERS

Consider the class of transfer functions of the form

$$H_0(z) = \frac{A_0(z^2) + z^{-1}A_1(z^2)}{2} \quad (11)$$

$$H_1(z) = H_0(-z) = \frac{A_0(z^2) - z^{-1}A_1(z^2)}{2} \quad (12)$$

$$A_i(z^2) = \prod_{j=1}^{P_i} \frac{\alpha_{i,j} + z^{-2}}{1 + \alpha_{i,j}z^{-2}}, i = 0, 1 \quad (13)$$

Properties of these filters are well-known [6, 7]. It is possible to design exceptionally sharp PS-QMF-IIR filters with high stop-band attenuation by using a small number of all-pass coefficients. For example, the amplitude characteristics of (11) for $P_0 = 6$, $P_1 = 5$, $\theta_s = 1.6085$ rad. is shown in Figure 3 [3]. Compared to prototype AC-QMF-FIR or PR-QMF-FIR filters, PS-QMF-IIR filters are much closer to an ideal brick-wall filter but, of course, they have non-linear phase characteristics which we shall briefly discuss in Section 4.

3 TWO-BAND AEC WITHOUT CCI

3.1 AC-QMF-FIR Filter Banks

Let $H(z) = \sum_{k=0}^N h_k z^{-k}$ (N :odd) be a *linear-phase* low-pass filter. We choose $H_0(z) = H(z)$, and $H_1(z) = H(-z)$. For sufficiently long filters with unity pass-band gain,

$$\det[\mathbf{H}_m(z)] = H^2(z) - H^2(-z) \approx z^{-N} \quad (14)$$

For no CCI, we use $C_{0,1}(z) = 0$ and $C_{1,0}(z) = 0$, and choose $G_0(z) = 2H_0(z)$ and $G_1(z) = -2H_0(-z)$ for aliasing cancellation. Furthermore, if N is sufficiently long, $H_0(z)$ is not far from being lossless [2]. Under these conditions, the residual error signal is

$$\begin{aligned} z^{-N}E(z) &\approx -H(z)H(-z) \\ &[S(z) - S(-z)][2H(z)H(-z)X(z) + X(-z)] \end{aligned} \quad (15)$$

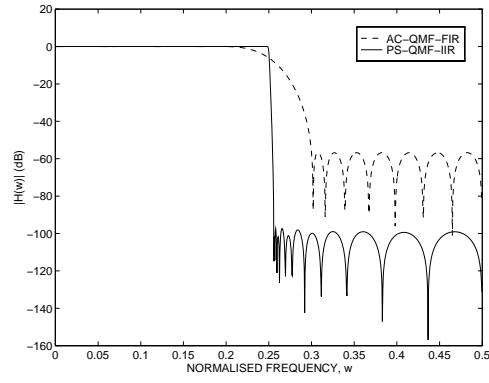


Figure 3: Amplitude spectra of the PS-QMF-IIR and AC-QMF-FIR ($N = 31$) filters, $\omega = \theta/2\pi$.

3.2 PS-QMF-IIR Filter Banks

As before we choose $H_0(z) = H(z)$, $H_1(z) = H(-z)$. Using (11)-(13) in (3), we have

$$\det[\mathbf{H}_m(z)] = H^2(z) - H^2(-z) = z^{-1}A_0(z^2)A_1(z^2) \quad (16)$$

Note that, unlike (14), (16) is not an approximation. If we use $C_{0,1}(z) = C_{1,0}(z) = 0$, (16) and choose $G_0(z) = 2H(z)$ and $G_1(z) = -2H(-z)$ for aliasing cancellation

$$\begin{aligned} z^{-1}A_0(z^2)A_1(z^2)E(z) &= H(z)H(-z)[S(-z) - S(z)] \\ &(2H(z)H(-z)X(z) + [H^2(z) + H^2(-z)]X(-z)) \end{aligned} \quad (17)$$

or, on the unit circle

$$\begin{aligned} e^{-j\theta}A_0(2\theta)A_1(2\theta)E(\theta) &= H(\theta)H(\theta - \pi)(S(\theta - \pi) - S(\theta)) \\ &(2H(\theta)H(\theta - \pi)X(\theta) + [H^2(\theta) + H^2(\theta - \pi)]X(\theta - \pi)) \end{aligned} \quad (18)$$

$H(z)$ is a highly selective prototype filter with very narrow transition band and high stop-band attenuation. Furthermore, it has a real impulse response; $H(-\theta) = H^*(\theta)$. Therefore, we make the following approximation

$$\Psi(\theta) \triangleq H(\theta)H(\theta - \pi) \approx |H(\pi/2)|^2(\delta(\theta - \pi/2) + \delta(\theta + \pi/2)) \quad (19)$$

where $\delta(\theta)$ is the impulse function which is quite convenient because this is the closest we can get to an ideal filter. The magnitude of $\Psi(\theta)$ for the IIR filter in Figure 3 is shown in Figure 4. Note that, from (11) $|H(\pi/2)|^2 = 1/2$ and $H^2(\theta) + H^2(\theta - \pi) = 0$ at $\theta = -\pi/2, \pi/2$. When (19) is valid, the right-hand side is non-zero only at $\theta = -\pi/2, \pi/2$ and for these values, $A_0(\pi) = (-1)^{P_0}$, $A_1(\pi) = (-1)^{P_1}$. Therefore, in the time-domain we have

$$\begin{aligned} e_n &\approx \frac{1}{\pi}(-1)^{P_0+P_1}\text{Im}[S(\pi/2)] \\ &(\text{Re}[X(\pi/2)]\cos(\pi/2n) - \text{Im}[X(\pi/2)]\sin(\pi/2n)) \end{aligned} \quad (20)$$

Unless $\text{Im}[S(\pi/2)] = 0$, which is not realistic considering arbitrary nature of the acoustic echo path, (20) is non zero. Thus, the residual error is a sinusoidal waveform. When $x_n = 0$, the error is also zero (when there is silence in the

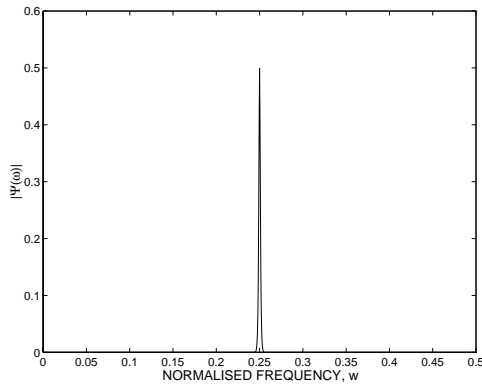


Figure 4: $\Psi(\theta)$ for the IIR filter in Figure 3, $\omega = \frac{\theta}{2\pi}$.

loudspeaker, the residual echo is also silent). On the other hand, when there is speech activity at the far-end, *tonal components* appear in the residual echo signal.

We now carry out similar investigations for AC-QMF-FIR decomposition to characterise the nature of the residual error signal in the absence of CCI. For this purpose it is necessary to approximate $\Psi(\theta)$. Let us denote the stop-band frequency of $H(z)$ by θ_s . An accurate approximation for $\Psi(\theta)$ around $\theta = \pi/2$ would then be a raised cosine. In the interval $\pi - \theta_s < \theta < \theta_s$, we have

$$\Psi(\theta) \approx \frac{1}{8} \left(1 - \cos\left(\frac{2\pi}{\pi - 2\theta_s}(\theta - \theta_s)\right) \right) e^{-j2N\theta} \quad (21)$$

The magnitudes of $\Psi(\theta)$ and (21) are shown in Figure 5. If

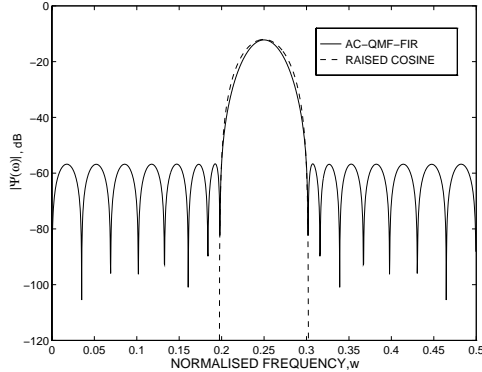


Figure 5: The magnitudes of $\Psi(\theta)$ and (21) for the AC-QMF-FIR filter in Figure 3, $\omega = \theta/2\pi$, $\theta_s = 1.8908$ rad.

we carry out similar operations as before, we have

$$e_n \approx -2f_n * (\sin^2(\pi/2n)s_n) * (2f_n * x_{n-N} + (-1)^n x_n) \quad (22)$$

where $*$ denotes the linear convolution operation and

$$f_n = \frac{1}{4\pi} \cos(\pi/2n) \sin((\theta_s - \pi/2)n) \left(\frac{1}{n} - \frac{n}{n^2 - \left(\frac{2\pi}{\pi - 2\theta_s}\right)^2} \right) \quad (23)$$

is a rapidly decreasing *sinc* type function. In an FIR based approach, if θ_s is close to π , f_n becomes shorter in time-domain but the aliasing bandwidth increases which is clearly

undesirable. If on the other hand, θ_s is close to $\pi/2$, $H(z)$ becomes closer to an ideal brick-wall filter, similar to the PS-QMF-IIR filter. Consequently, f_n becomes longer and in the limit e_n in (22) will be a cosine type waveform.

4 NOTCH FILTERING

The time-domain characteristics of $\Psi(\theta)$ indicate the lengths of $C_{0,1}(z)$ and $C_{1,0}(z)$ that must be identified. If $H(z)$ is an FIR filter, reasonably short length cross-adaptive filters can be used. The decrease in convergence speed is due to the adaptive nature of this solution.

For the PS-QMF-IIR filter in Figure 3, $F^{-1}\{\Psi(\theta)\}$ is at least one order of magnitude longer. Therefore, we can not really use cross-adaptive filters to remove the effect of aliasing. However, since $\Psi(\theta)$ is much more coherent for a typical PS-QMF-IIR filter, notch filters can be used to attenuate the input of the analysis bank around sub-band edges so that $\Psi(\theta) \approx 0$. Note that, unlike cross-adaptive filtering, the solution of notch filters is a deterministic one and therefore convergence speed of the AEC is not affected.

For low computational burden, we use an IIR notch structure based on all-pass networks [4]. Let us start with the prototype low-pass filter

$$\tilde{N}(z) = \frac{1}{2} \left(\frac{\alpha_{0,1} + z^{-2}}{1 + \alpha_{0,1}z^{-2}} + z^{-1} \frac{\alpha_{1,1} + z^{-2}}{1 + \alpha_{1,1}z^{-2}} \right) \quad (24)$$

which is a special case of (11) for $P_0 = P_1 = 1$. By using an all-pass low-pass to band-stop frequency transformation [1], the notch filter $N(z)$ can be obtained as

$$N(z) = \frac{1}{2} \left(N_0(z) + \frac{\zeta + z^{-2}}{1 + \zeta z^{-2}} N_1(z) \right) \quad (25)$$

where

$$N_i(z) = \frac{\gamma_{i,2} + \gamma_{i,1}z^{-1} + z^{-2}}{1 + \gamma_{i,1}z^{-1} + \gamma_{i,2}z^{-2}} \frac{\gamma_{i,2} - \gamma_{i,1}z^{-1} + z^{-2}}{1 - \gamma_{i,1}z^{-1} + \gamma_{i,2}z^{-2}} \quad (26)$$

$i = 0, 1$. A prototype low-pass filter of the form (24) with $\alpha_{0,1} = 0.402117$ and $\alpha_{1,1} = 0.853158$ is spectrally transformed as described above. The all-pass coefficients in (25)-(26) are $\zeta = 0.806325$, $\gamma_{0,1} = 0.184887$, $\gamma_{0,2} = 0.913338$, $\gamma_{1,1} = 0.210793$ and $\gamma_{1,2} = 0.983340$. The corresponding amplitude spectrum is in Figure 6. In the sub-band AEC

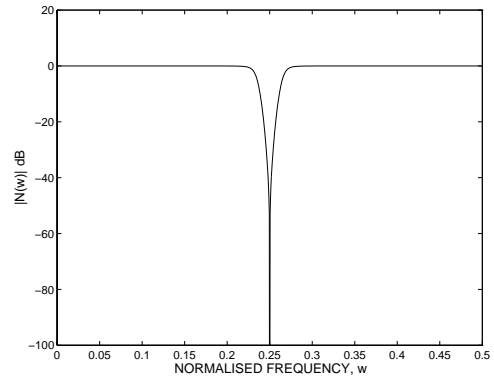


Figure 6: Amplitude spectrum of the notch filter.

system in Figure 2, there are several candidate positions that

notch filters can be inserted. It is appropriate to put notch filters either at 1 or 3 or 2 and 3. If notch filters are put at 2 and 3, the residual echo signal will be

$$z^{-1}A_0(z^2)A_1(z^2)E(z) = H(z)H(-z)N(z)[S(-z) - S(z)] \\ (2H(z)H(-z)X(z) + [H^2(z) + H^2(-z)]X(-z)) \quad (27)$$

Therefore, the coherent part of $H(\theta)H(\theta - \pi)$ is attenuated by $N(\theta)$. Notch filtering is also a partial solution to the non perfect phase reconstruction of the PS-QMF-IIR filter banks, since the part of the spectrum where phase distortion occurs most is attenuated.

5 SIMULATIONS

The loudspeaker signal is zero-mean, white and Gaussian with unity power. The echo-path impulse response of a car environment (256 taps) is used to generate the echo signal. A fast QR-Lattice adaptive algorithm is used in both sub-bands with 128 adaptive coefficients. The resulting residual echo signal and its amplitude spectrum are respectively shown in Figures 7 and 8 with and without notch filtering. When there is no notch filtering, there is a tonal component at $\theta = \pi/2$. When notch filtering is used, the tonal component is suppressed significantly. Generally, the performance is improved at all frequencies.

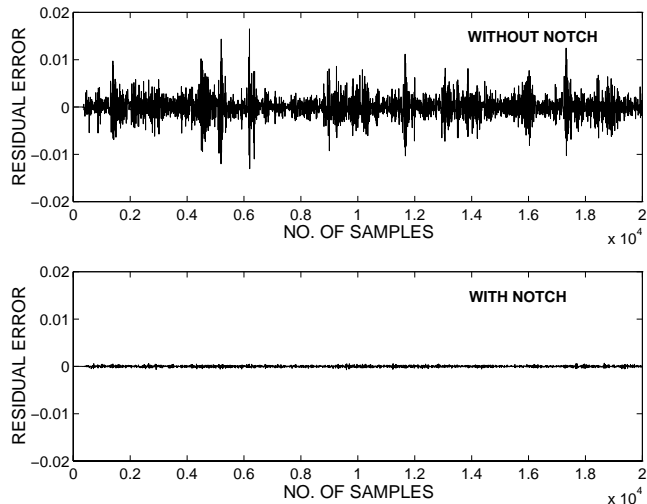


Figure 7: Residual echo signals with and without notch filtering.

Real speech recorded in a car environment is also used as the loudspeaker signal. The results in Table 1 are averages over several recordings. In separate experiments, it is

Filter Bank	Av. ERLE (dB)	TIC (msec.)
AC-QMF-FIR	23.51	32.00
PS-QMF-IIR	21.74	32.00
PS-QMF-IIR+notch	24.81	32.00

Table 1: Echo Return Loss Enhancement (ERLE), and Time of Convergence to 10dB ERLE (TIC).

observed that such notch filters do not create audible distortion of the near-end speech.

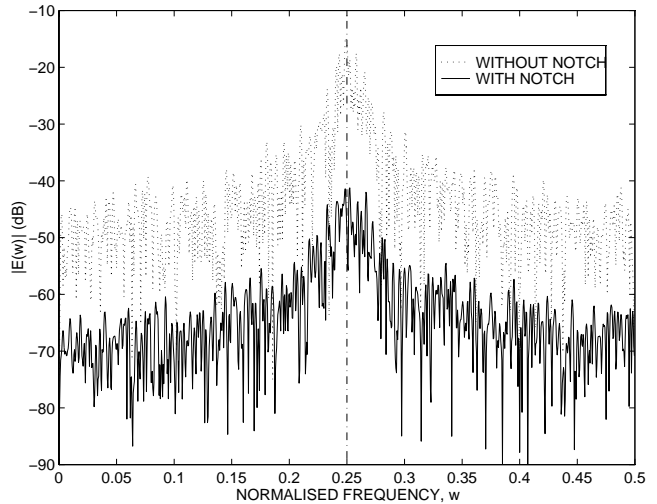


Figure 8: Amplitude spectrum of the residual error signal with and without notch, $\omega = \frac{\theta}{2\pi}$.

6 CONCLUSIONS

PS-QMF-IIR and AC-QMF-FIR filters are studied in the context of AEC. The properties of the residual error are investigated when there is no CCI. The tonal artifacts that appear while using PS-QMF-IIR filters are suppressed efficiently by using notch filters. The proposed scheme delivers the desired performance at low computational complexity.

References

- [1] A. G. Constantinides. Frequency transformations for digital filters. *IEE Proc.*, 117(8):1585–1590, Aug. 1970.
- [2] A. Gilloire and M. Vetterli. Adaptive filtering in sub-bands with critical sampling: Analysis, experiments and application to acoustic echo cancellation. *IEEE Trans. Sig. Proc.*, 40(8):1862–1875, Aug. 1992.
- [3] O. Tanrikulu, B. Baykal, A. G. Constantinides, J. A. Chambers, and P. A. Naylor. Finite-precision design and implementation of all-pass polyphase networks for echo cancellation in sub-bands. In *ICASSP-95*, pages 3039–3042, May 1995.
- [4] O. Tanrikulu. *Adaptive signal processing algorithms with accelerated convergence and noise immunity*. PhD thesis, Imperial College, 1995.
- [5] O. Tanrikulu, B. Baykal, A. G. Constantinides, and J. A. Chambers. Residual echo signal in critically sampled sub-band acoustic echo cancellers with IIR and FIR filter-banks. *submitted to IEEE Trans. Sig. Proc.*, 1995.
- [6] P. P. Vaidyanathan. *Multi-rate Systems and Filter Banks*. Englewood Cliffs, NJ: Prentice-Hall, 1993.
- [7] R. A. Valenzuela and A. G. Constantinides. Digital signal processing schemes for efficient interpolation and decimation. *IEE Proc.*, 130(6):225–235, Dec. 1983.